A new Ti/H phase transformation in the H_2^+ titanium alloy studied by x-ray diffraction, nuclear reaction analysis, elastic recoil detection analysis and scanning electron microscopy

2002 J. Phys.: Condens. Matter 14 11605

(http://iopscience.iop.org/0953-8984/14/45/304)

INSTITUTE OF PHYSICS PUBLISHING JOURNAL OF PHYSICS: CONDENSED MATTER

J. Phys.: Condens. Matter **14** (2002) 11605–11614 PII: S0953-8984(02)39166-5

A new Ti/H phase transformation in the H_2^+ titanium alloy studied by x-ray diffraction, nuclear reaction analysis, elastic recoil detection analysis and scanning electron microscopy

T Wang[1,2,3], F Eichhorn[1], D Grambole[1], R Grötzschel[1], F Herrmann[1], U Kreissig[1] and W Möller[1]

[1] Forschungszentrum Rossendorf eV Institut für Ionenstrahl physik und Materialforschung, PF 510119, D-01314 Dresden, Germany
[2] Institute of Modern Physics, Chinese Academy of Sciences, Lanzhou 73000, People's Republic of China

E-mail: t.wang@fz-rossendorf.de and tswang@ns.lzb.ac.cn

Received 4 July 2002, in final form 2 October 2002
Published 1 November 2002
Online at stacks.iop.org/JPhysCM/14/11605

Abstract

The titanium hydrogenation process in the H_2^+ implanted Ti225 titanium alloy has been studied in this work. The Ti/H phase transformation from hydrogen solid solution (hcp) to gamma phase titanium hydride ($TiH(\gamma)$) with a primitive tetragonal structure and then to a titanium dihydride ($TiH_2(x)$) with a body centred tetragonal structure has been characterized by x-ray diffraction, nuclear reaction analysis and elastic recoil detection analysis. This process is very different from the usual hydrogenation mechanism, in which the delta phase titanium dihydride ($TiH_2(\delta)$) with a face centred cubic structure is always involved. Both of the $TiH(\gamma)$ and $TiH_2(x)$ are rare phases, which are formed under extreme conditions. The $TiH(\gamma)$ was considered to be a metastable phase in low hydrogen concentration titanium, and the $TiH_2(x)$ phase has not yet been notated in the present Ti/H phase list. The characteristics of the $TiH_2(x)$ are unclear, but it is very stable at room temperature and exists as a mixture state with the titanium. A saturated fraction of the hydride to titanium phase has been obtained as about 15% (H/Ti $\sim$ 0.3) in a H_2^+ implanted sample.

1. Introduction

Titanium and its alloys have many outstanding physical and chemical superiorities, hence, they have been widely used as important structural metals in various engineering applications, ever since the commercial titanium metal was produced in 1946. Because of the strongly active behaviour of hydrogen in titanium and its alloy, the titanium hydrogenation mechanism is very

[3] Author to whom any correspondence should be addressed, financially supported by Max-Planck Society.

complex. A series of studies to understand the mechanism of titanium hydrogenation and titanium hydrides have been conducted in bulk metals [1, 2]. However, the previous works are mostly concerned with either the hydrogen embrittlement [3–5] or the hydrogen storage [6–9] problems. The titanium hydrogenation in very low H concentration (embrittlement) and extremely high H concentration (storage) has been studied extensively; however there are very limited studies on the Ti hydrogenation with a intermediate H concentration, encountered in the ion beam implantation and some corrosion studies [1, 10–12].

In order to improve the surface properties of titanium metals, ion beam implantation and plasma bombardments are often used. However, hydrogen contamination has been observed in many ion beam and plasma implantation experiments in titanium [10–12]; it could significantly influence both the quality of the surface modification and the mechanical properties of the metal. The mechanism of hydrogen accumulation induced by ion beam implantation is still unclear. Therefore, a study of the hydrogenation mechanism in a hydrogen implanted titanium sample is essential to understand both the ion beam enhanced H accumulation and the hydrogenation mechanism in an intermediate H concentration titanium.

Compared to other hydrogen loading methods, the ion implantation has the advantage of loading the hydrogen into a required location with a controlled dose in the sample by selecting the ion energy and implantation dose. The micro-mechanism of the hydrogenation could therefore be easily investigated by characterizing the hydrogen concentrated region. In this work, the ion beam analyses are applied to determine the hydrogen concentration and depth distribution, and the x-ray diffraction (XRD) is used to characterize the hydride phase transformation versus the hydrogen concentration. The surface topography was investigated by high resolution scanning electron microscopy (SEM).

2. Experimental procedure

The sample material in this study is Ti225 titanium alloy, which consists of titanium (95 at.%), aluminium (2 at.%), vanadium (2 at.%), zirconium (<1.0 at.%) etc elements. It is characterized as alpha phase metal at room temperature and has a hexagonal close-packed (hcp) crystal structure with lattice constants $a = b = 2.9505$, $c = 4.6826$, unit-cell volume of 35.28 Å^3. The size of all the samples used in this study was 8 mm × 8 mm × 0.3 mm. All of them were cut from the same plate and cleaned chemically with the standard chemical etching process for titanium prior to the hydrogen implantation.

The hydrogen implantation was performed using the 200 kV implantation facility at FZ Rossendorf. Samples were implanted by H_2^+ at a constant energy of 25 keV amu^{-1} with varied doses from 2×10^{15} to 6×10^{17} H cm^{-2}. During all the implantations the target temperature was monitored with a thermocouple on the corner of the sample and maintained to be below 60 °C by cooling water. Samples were stored in air after implantation.

Hydrogen-related phase transformation and the textural change in the samples were characterized by XRD. A copper anode is employed in the XRD facility. The x-ray wavelengths from the copper anode are 1.540 560 and 1.544 390 Å, respectively. The entrance slit and sample slit were set as 1.0 mm between anode and sample. The x-rays' incident angle was 1.5° to the sample surface; therefore, the measuring depth was around 1 μm. The sample was rotated during the measurement at a constant velocity. The diffraction was measured in the 2θ angle ranges from 37° to 45° and from 56° to 62°. The interesting diffraction peaks from titanium and titanium hydrides are mostly located in these two angular ranges. The XRD diagrams were analysed with the JCPDS-PDF data bank.

The resonant nuclear reaction analysis (NRA) with ^{1}H(^{15}N$^+$, $\alpha\gamma$)^{12}C reaction and heavy ion elastic recoil detection analysis (ERDA) have been used to study the H concentration

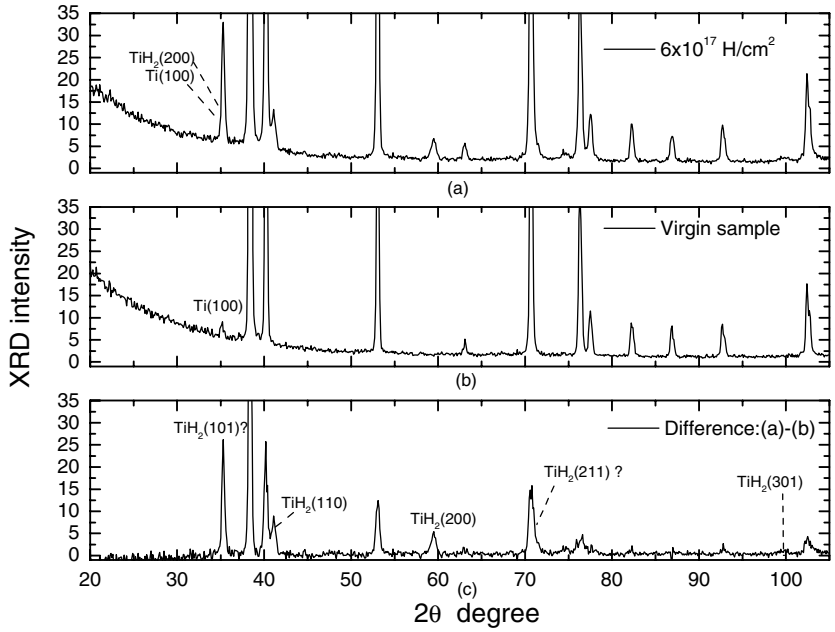

Figure 1. XRD diagrams of the sample implanted with 6×10^{17} H cm^{-2} (a), the virgin sample (b) and the net difference between the two (c).

and depth profile. Both analyses were performed at the 2 × 5 MV tandem accelerators at Rossendorf. The H depth profiles in the titanium samples have been obtained by NRA with a depth resolution of 5 nm. The integral H concentration in the near surface region of the samples was determined by heavy ion ERDA with 35 MeV Cl^{7+}.

The H planar distribution was measured by microprobe-scanning elastic recoil detection analysis (micro-ERDA) at the 2 × 3 MV tandem accelerator at Rossendorf [13]. A silicon ion beam (Si^{5+}) at 16 MeV was employed as the incident beam. A beam spot with diameter less than 5 μm was obtained, which resulted in the lateral resolution in the experiment of about 5 (vertical) ×15 (horizontal) μm^2 due to the 20° incidence angle. The effective measuring depth for H in the titanium sample is about 350 nm. The two-dimensional contour map of the H planar distribution was achieved by X–Y-scan of the micro-beam.

A high resolution SEM (DSM 962) at FZR was used to observe the surface topography of samples.

3. Experimental results

3.1. XRD study of the change of material structure

The XRD diagrams in the H_2^+ implanted samples, the virgin sample and the subtraction of both are shown in figure 1. The diffraction peaks (002) and (101) of hcp titanium are found at $2\theta = 38.4°$ and 40.2° in the diagram. Some new peaks are seen at $2\theta = 36°$, 41°, 60°, 71° and 100° in figure 1(c). The peaks are identified to be titanium dihydride (TiH_2 JCPDS-PDF 9-371) interferences (101) (35.892°), (110) (40.991°), (200) (59.599°), (211) (70.785°) and (301) (99.40°), respectively. This titanium dihydride has a body centred tetragonal (bct) structure (TiH_2 JCPDS-PDF 9-371) [15].

In the XRD diffraction diagram of the samples implanted with a low dose, two peaks at $2\theta = 39.5°$ and 43° are found. They are identified to be titanium hydride (TiH JCPDS-PDF

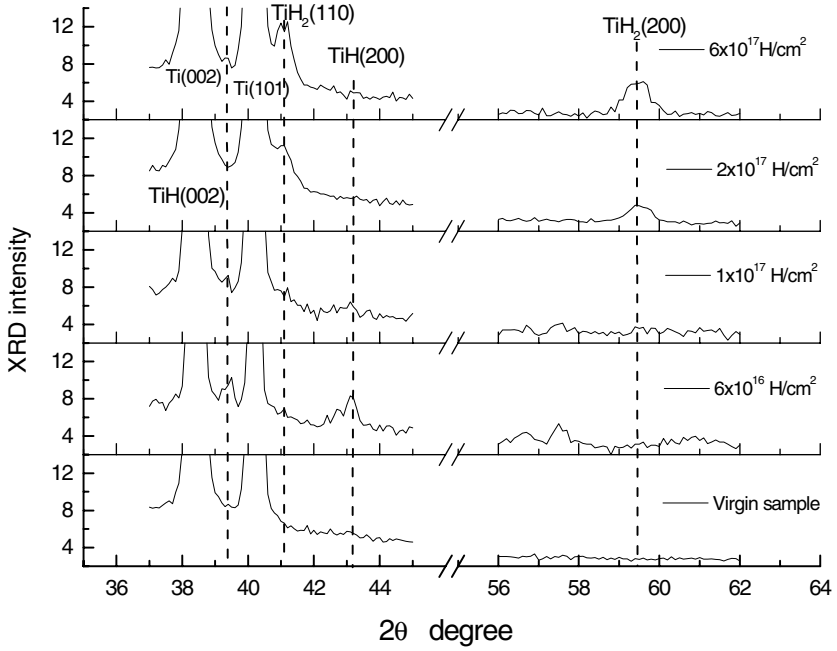

Figure 2. The comparison of important XRD peaks from TiH(γ) and TiH_2(x) matrices versus H implantation.

40-1244) interferences (002) (39.348°) and (200) (43.059°), respectively. This TiH_1 is defined as the γ phase of titanium hydride (TiH(γ)) with a tetragonal (primitive) matrix [1, 14].

A comparison of the interesting regions of the XRD diagrams in samples implanted with varied fluences is shown in figure 2. It is seen that the crystal structure changes in the samples with the variation of the implantation dose, as characterized by the XRD. Only some traces of diffraction peaks in TiH(γ) are found in the virgin sample, but TiH(γ) peaks in the diagram in the sample implanted with 6×10^{16} H cm^{-2} are evident (figure 2). In the sample implanted with 1×10^{17} H cm^{-2} the TiH(γ) peaks decrease, and an increase at the TiH_2 peaks' positions is observed. Furthermore, only peaks from the TiH_2 phase can be seen in the sample implanted with 1×10^{17} H cm^{-2}; the TiH_2 peaks in the sample implanted with 6×10^{17} H cm^{-2} are very clear, but the peaks from the TiH(γ) phase almost vanish in the same diagram.

The change of the diffraction intensities of the TiH(γ) and TiH_2 versus the integrated H precipitation shows such a trend: the XRD intensity in the TiH(γ) phase decreases, while it increases in the TiH_2 phase with the increase of the H precipitation. The ratios between the different diffraction peaks in the same matrix keep almost constant in the measuring uncertainties within the experimental uncertainty.

The XRD measurement on the same samples was repeated 230 days after the first measurement. No evident change has been noticed, confirming the stability of the hydride formation at room temperature.

3.2. Hydrogen precipitation and distribution

The depth profiles of H concentration are shown in figure 3. They correspond to various H doses in XRD diagrams (figure 2). A surface hydrogen concentration is found in the virgin sample. Most of the implanted hydrogen is found in the near surface region but not around

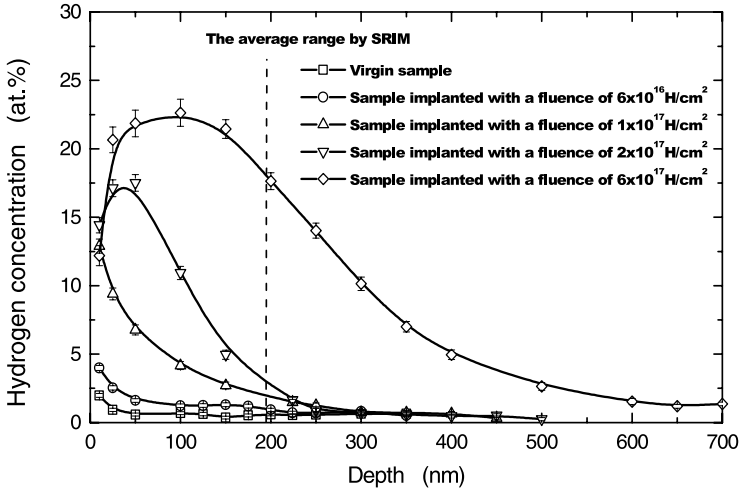

Figure 3. Depth profile of H concentration versus implantation dose.

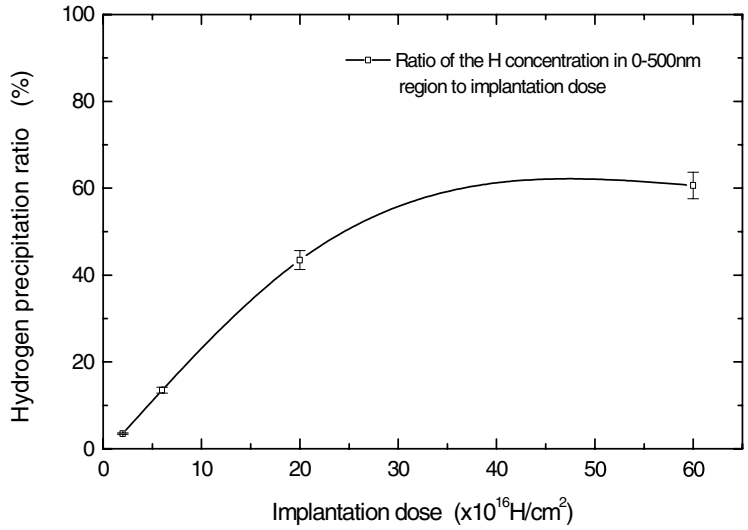

Figure 4. H precipitation versus implantation dose.

the implantation range in the samples. A saturated hydrogen concentration with a value about 23 at.% is obtained in the sample implanted with 6×10^{17} H cm^{-2} (figure 3). Instead of the increase of H concentration, the H precipitation region extends to deep inside the sample, while the saturation is reached. A significant H loss is found on the surface of the samples implanted with a dose above 1×10^{17} H cm^{-2}.

The integrated precipitation of implanted H in the near surface region (0–500 nm) of the sample is determined by the ERDA measurement. The H precipitation is found to increase nonlinearly with the implantation dose (figure 4). The ratio increases almost directly, while the dose is lower than 2×10^{17} H cm^{-2}, and then increases gradually for dose above 2×10^{17} H cm^{-2} and finally saturates at about 60% in the region after 4×10^{17} H cm^{-2}.

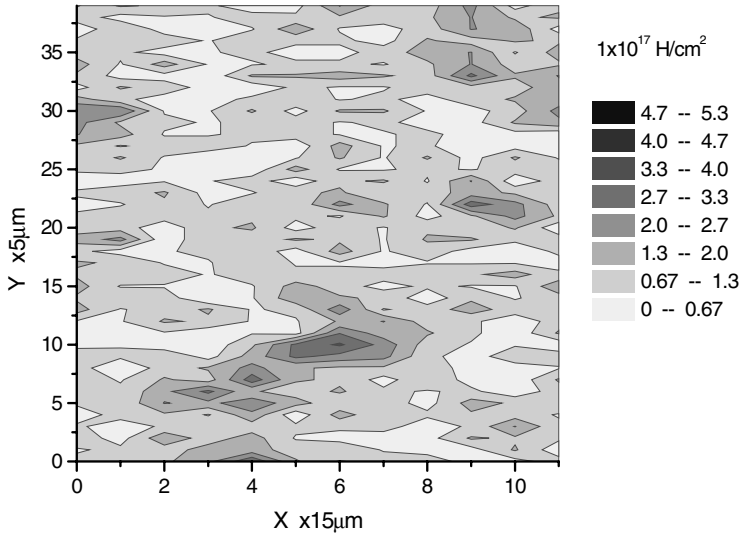

Figure 5. Contour map of H concentration in the sample implanted with 1×10^{17} H cm^{-2} measured by micro-ERDA.

The H planar distribution obtained by scanning micro-ERDA in the sample implanted with a dose of 1×10^{17} H cm^{-2} is presented in figure 5. An inhomogeneous H distribution is seen in the contour map. The inhomogeneity factor (on the right of the figure) is defined as the ratio of H concentration of each pixel to the average H concentration value of all 480 pixels. A significant contrast is found by comparing the high H concentration regions and low H concentration region.

The corresponding SEM picture of the same sample is shown in figure 6. Many different sized spheres distribute inhomogeneously on the sample surface demonstrate the formation of a new phase. A significant high concentration of the new phase is found in a region with size of a few micrometres.

4. Discussion and analysis

The hydrogen in titanium is very active [1, 16, 17]. The titanium hydrogenation process is therefore very complicated and strongly depends on temperature, pressure, concentration and ingression methods etc. More than six hydride phases have been found in previous works. The notation of titanium hydrides, which is almost universally accepted today, is listed in table 1 [1, 14, 15].

As usual in the titanium hydrogenation mechanism, the H atoms dissolve in a low H concentration titanium sample as α solid solution. If the H concentration is above the H solubility, which is about 20–22 ppm by wt.% or 0.12 at.% at room temperature for pure titanium [16], the delta phase hydride ($TiH_2(\delta)$) should be formed and exists as a mixture with the α solution in the titanium until 57 at.% [1]; then a single $TiH_2(\delta)$ phase material is formed. In the stoichiometric TiH_2 (H/Ti >1.98), the $TiH_2(\delta)$ phase transforms to $TiH_2(\varepsilon)$ phase at low temperature (<20 °C).

Unlike the other H loading methods, e.g. gaseous H absorption and electrolytic hydrogenation [1], by implantation, the energetic hydrogen ions (H_2^+) ingress into the sample by impact and finally stop at a similar depth; the energy of ions is deposited along the tracks

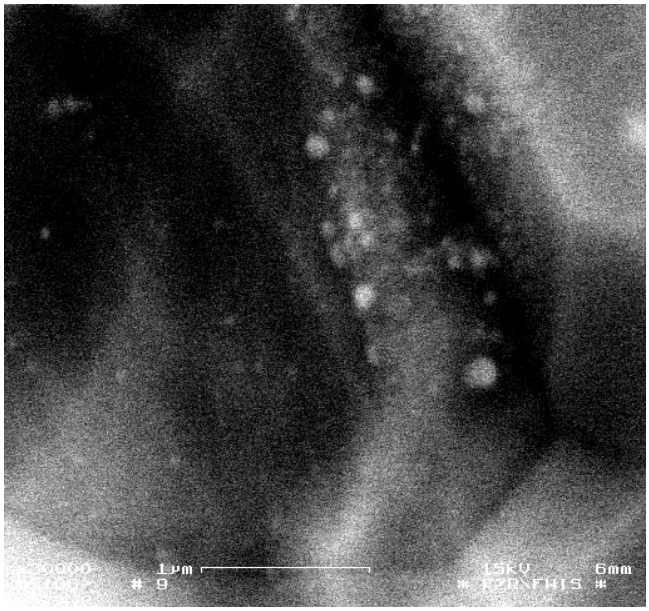

Figure 6. SEM topography of a sample surface.

Table 1. List of titanium hydrides (*hydride observed in this work but not yet notated in the present Ti/H phase list).

Ti/H phases	Matrix	$a = b$/ Å	c/Å	V per atom (Å^3)	$\Delta V/V$ (%)	H/(H+Ti): at.% (x in TiH_x)	Note
α	hcp	2.951	4.683	17.65	0	<0.12	Solid solution
β	bcc	3.30	3.30	18.13	2.5	∼12(0.14)	$T > 883$°C
$TiH(\gamma)$	tetra.	4.199	4.576	20.17	14.3	1–3(<0.03)	Meta-stable
$TiH_2(\delta)$	fcc	4.44	4.44	21.88	24.0	<55(1.22)	Mix. with α phase
						>55(1.22)	Single phase
$TiH_2(\varepsilon)$	fct	4.528	4.279	21.93	24.2	∼66(1.94)	$T < 20$ °C
$TiH_x(\omega)$	bcc	4.620	2.828	∼	−14.7	(0.33)	P: 42–60 kbar
	Hex. distorted						
TiH_x	fcc	A:4.34	4.02	18.23	3.3	(0.71)	Formed at 45–65
	Orth. distorted	b:4.18					kbar, 555–730 K;
							Quenched <90 K
$TiH_2(x)$*	fct	4.42	4.18	20.35	15.3	>3%	This work
	(bct)	(3.12)	(4.18)				

and causes a significant number of defects and dislocations in the implantation region, and a significant inner strain difference between the implanted region and the unimplanted region is therefore induced. The H diffusion and hydrogenation following the implantation occurs inside the sample under a complex solid environment and is much more complicated than the other hydrogenation processes.

As seen in figures 3 and 4, the implanted H precipitates in the near surface region, where the inner strain is inhomogeneous. The α solid solution of implanted H can be therefore confirmed in samples with a low H concentration. Since the sample material used in this work is an α phase titanium alloy, the H solubility is somewhat higher than that in pure titanium

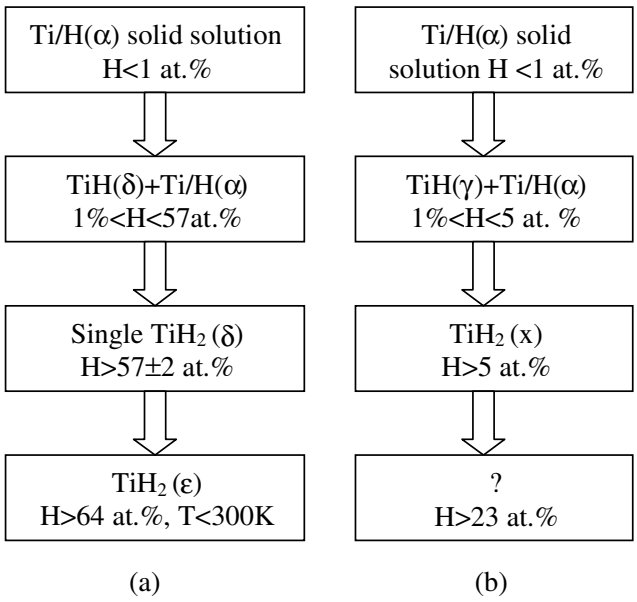

Figure 7. Schematics of the phase transformation in two hydrogenation procedures: (a) common hydrogenation; (b) hydrogenation in an implanted sample.

due to the existence of other elements, and is estimated to be around 1 at.% according to the experimental data. The TiH(γ) diffraction is also found in the virgin sample, but it is considered to be from the surface concentration, which is higher than the solubility due to the surface effect (figure 3). With the help of the XRD results, the phase transformation from α solid solution to TiH(γ) and further to $TiH_2(x)$ is therefore established. The comparison of the two hydrogenation processes is described as the following.

It is shown in figure 7 that, instead of $TiH_2(\delta)$, TiH(γ) is formed first in the sample implanted with low doses. The TiH(γ) was considered to be a meta-stable hydride phase precipitated on cooling from the α solution in titanium with 1–5 at.% concentration [1, 16]. A significant amount of the TiH(γ) phase is found in the sample implanted with 6×10^{16} H cm^{-2}, in which the H concentration is at a few atomic per cent level (see figure 3). After the TiH(γ) phase, titanium dihydride phase TiH_2(x) starts to be formed as soon as the H concentration exceeds 5 at.%. At the same time, the TiH(γ) phase decreases and the TiH_2(x) grows gradually with the increase of H implantation (see figure 2). Both phases are observed in the sample implanted with 1×10^{17} H cm^{-2}. In the sample implanted with a dose of 6×10^{17} H cm^{-2}, only $TiH_2(x)$ can be observed by XRD. This implies that almost all of the TiH(γ) phase transforms into $TiH_2(x)$ (see figure 2). However, the fraction of $TiH_2(x)$ saturates at about 15%, which is derived from the H concentration saturation value of 23 at.%. Strong diffraction on the titanium matrix is also seen in figure 1. Thus, the $TiH_2(x)$ exists as a mixture with the titanium phase. Then a strain is necessary for material equilibrium in the surrounding Ti matrix. This strain is inhomogeneous over the matrix volume and broadens the Ti reflections (see figure 1). The inhomogeneous H planar concentration measured by micro-ERDA (see figure 5) and the SEM picture (see figure 6) show the inhomogeneous mixture of the phases.

On the basis of our XRD results, the $TiH_2(x)$ phase appears to be a little-known phase first reported by Jaffe in 1956 [15]. It was claimed to be a bct matrix with $a = b = 3.12$ Å and $c = 4.18$ Å (JCPDS-PDF 9-371), which was indicated to be equivalent to a face-centred-

tetragonal complex with $a = 4.42$ Å and $c = 4.18$ Å [16]. However, this phase has not been mentioned or notated up to now. The characteristics of this phase are almost unknown.

Comparing the two hydrogenation processes, the reaction environments are rather different. The common hydrogenation occurs usually from the surface gradually to deep inside. At the same time, the inner strain in the sample is homogenous. On the surface, only the bond energy from one side of the lattice needs to be overcome to form the hydride matrix. Thus, with the help of the surface strain, a new phase matrix may be formed rather easily. On the base of the existing new matrix, a further development of the phase should also be relatively easy. However, in an implanted sample, the H atoms are directly implanted into a limited region inside the bulk, and hence the structure change is strongly restricted by the surrounding titanium matrix. Hence, to form the hydride matrix in an implanted sample much more energy is needed than on the surface.

Each Ti atom in the α titanium matrix has only a volume of 17.65 Å^3. The volume per atom in most of the hydride matrices is larger than that in titanium (see table 1). Therefore, a volume swelling is involved in most of the titanium hydrogenation processes to form hydrides. The volume swellings during formation of TiH(γ), $TiH_2(\delta)$ and $TiH_2(x)$ are 14.3, 24.0 and 15.2%, respectively. Compared to the other phases, the volume swelling by the phase transformation from titanium to TiH(γ) is smallest. Thus it has the priority to occur at first in the sample, with the help of the defects and dislocations induced by ion implantation.

Since the TiH(γ) is a metastable Ti/H phase, it should be further transformed to another TiH_2 phase in some conditions. Two possible transformations are from TiH(γ) to $TiH_2(x)$ and from TiH(γ) to $TiH_2(\delta)$. The volume swellings involved in these two transformations are 0.9 and 8.5%, respectively. Otherwise, both TiH(γ) and $TiH_2(x)$ have the tetragonal matrix, and two of the three lattice constants decrease in their transformation. On the other hand, in the transformation from TiH(γ) to $TiH_2(\delta)$, two of the three lattice constants must extend significantly. Therefore, the transformation from TiH(γ) to $TiH_2(x)$ is most likely to occur following the increase of the H concentration in the implanted titanium sample.

The further phase transformation from $TiH_2(x)$ to $TiH_2(\delta)$ involves a great change of the cell volume; all three lattice constants should be enlarged to 4.44 Å, so it is very unlikely to occur. Thus, no $TiH_2(\delta)$ phase could be observed in this work. However, the H concentration saturated at 23 at.% in the implanted sample; hence, it cannot be proved whether the transformation from $TiH_2(x)$ to $TiH_2(\delta)$ could occur in a sample with a higher H concentration.

5. Conclusion

The hydrogenation mechanism in a H_2^+ implanted titanium sample is different from the common titanium hydrogenation mechanism. Two rare phases, TiH(γ) and $TiH_2(x)$, are found in the sample. The two-step phase transformation from H α-solid solution to TiH(γ) and then to $TiH_2(x)$ is confirmed by XRD, NRA, ERDA and SEM. The $TiH_2(x)$ phase is an unnamed phase, which has not been known well. However, it is stable at room temperature in the environments in implanted samples and exists as a mixture phase with titanium. A saturated phase fraction is found at about 15% in the high H concentration sample.

Acknowledgments

Dr E Richter from FZR is acknowledged for discussion and comments. Technical assistance from Mrs A Scholz, Mr G Winkler, F Ludwig etc, colleagues in different groups in FZR, is

gratefully acknowledged. Thanks go to Professor A Pathak for his reading of the manuscript. All samples were provided by the Nuclear Power Institute of China.

References

[1] Lewkowicz I 1996 Hydrogen metal system I *Solid State Phenomena* vol 49/50 ed F A Lewis and A Aladjem (Zurich: Trans Tech Publications) pp 239–79
[2] San-Martin A and Manchester F D 1987 *Bull. Alloy Phase Diag.* **8** 30–42
[3] Christ H-J, Decker M and Zeitler S 2000 *Metall. Mater. Trans.* A **31** 1507
[4] Abdul-Hamid O S and Latanision R M 1996 *Hydrogen Effects in Materials* ed A W Thompson and N R Moody (Warrendale, USA: TMS) p 205
[5] Puttlitz K J and Smith A J 1981 *Hydrogen Effect in Metal* ed I M Bernstein and A W Thompson (Warrendale, USA: Metallurgical Society of AIME) pp 427–34
[6] Zhang H and Kisi E H 1997 *J. Phys.: Condens. Matter* **9** L185–90
[7] Monnin C, Ballanger A, Sciora E, Steinbrunn A, Alexsandre P and Pelcot G 2000 *Nucl. Instrum. Methods Phys. Res.* B **453** 493–500
[8] Nakao S, Miyagawa S and Miyagawa Y 2000 *Nucl. Instrum. Methods Phys. Res.* B **169** 156–60
[9] Yakel H J 1958 *Acta. Crystallogr.* **11** 46
[10] Sugizaki Y, Furuya T and Satoh H 1991 *Nucl. Instrum. Methods Phys. Res.* B **59/60** 722
[11] Neu K *et al* 1994 *Nucl. Instrum. Methods Phys. Res.* B **89** 379
[12] Farshi M S *et al* 1997 *Nucl. Instrum. Methods Phys. Res.* B **127/128** 787
[13] Grambole D and Herrmann F 1999 *Nucl. Instrum. Methods Phys. Res.* B **158** 647
[14] Numakura H *et al* 1988 *Acta Metall.* **35** 2267
[15] Jaffe L D 1956 *J. Met.* **8** 861
[16] Wang T *et al* 2002 *Surf. Coat. Technol.* C **158/159** 139–45
[17] Paton N E, Hickman B S and Leslie D J 1971 *Metall. Trans.* **2** 608